Global Journal of Science Frontier Research: a
Physics and Space Science
Volume 16 Issue 4 Version 1.0 Year 2016
Type : Double Blind Peer Reviewed International Research Journal
Publisher: Global Journals Inc. (USA)
Online ISSN: 2249-4626 & Print ISSN: 0975-5896

Helical Iodine Chains inside Single-Walled Boron Nitride Nanotubes: Finding the Optimal Helical Radius and Helical Angles

By Zhen Yao, Chun-Jian Liu, Li-Qiang Feng, Yi Li & Zhong-Li Wu
Liaoning University of Technology

Abstract- The helicity of stable single, double, and triple helical iodine chains inside singe-walled boron nitride nanotubes is studied using the calculation of the systematic interaction energy. The results indicate that the optimal helical radius increases linearly with the radius of the tube. Hence, there is a constant distance between the I-chain and the tube's wall. The optimal helical angle depends on the inter-chain interaction. It is affected, however, by the tube's confinement effect: a small opt(φ) can be induced by large inter-chain for the same tube or a large tube for the same chain structure. The helicity of the encapsulated I-chains is insensitive to the tube's chirality but depends strongly on the tube diameter.

Keywords: peapod, nanotube, iodine chain.

GJSFR-A Classification : FOR Code: 020399p

Strictly as per the compliance and regulations of :

Helical Iodine Chains inside Single-Walled Boron Nitride Nanotubes: Finding the Optimal Helical Radius and Helical Angles

Zhen Yao [α], Chun-Jian Liu [σ], Li-Qiang Feng [ρ], Yi Li [ω] & Zhong-Li Wu [¥]

Abstract- **The helicity of stable single, double, and triple helical iodine chains inside singe-walled boron nitride nanotubes is studied using the calculation of the systematic interaction energy. The results indicate that the optimal helical radius increases linearly with the radius of the tube. Hence, there is a constant distance between the I-chain and the tube's wall. The optimal helical angle depends on the inter-chain interaction. It is affected, however, by the tube's confinement effect: a small opt(φ) can be induced by large inter-chain for the same tube or a large tube for the same chain structure. The helicity of the encapsulated I-chains is insensitive to the tube's chirality but depends strongly on the tube diameter.**

Keywords: peapod, nanotube, iodine chain.

I. Introduction

The synthesis and characterization of new one-dimensional (1-D) crystal structures with novel properties are common research areas in the worldwide scientific community [1, 2]. It is clear that the unique hollow structure of macromolecules like nanotubes and zeolite molecules provides an ideal opportunity to create new and well-defined 1-D molecular/atomic structures [3, 4]. Various peapod structures that use nanotube packing of molecules or atoms have been studied in both experiments and theory [5-9]. For example, single-walled carbon nanotube (SWCNT) hosts can greatly enhance the thermal stability of encapsulated C_{60} molecules compared with their bulk structures [10]. Upon high temperature annealing, the decomposed ferrocene molecules inside SWCNTs can produce another interior tube, which represents a new route for material design [7, 11]. Theoretical studies indicate that the distance between host and guest molecules is responsible for the stability and electronic hybrid properties of the peapod system [12-14]. Moreover, different achiral and chiral phases, such as the 1-D linear chain, the 2-D zigzag phase, and the 3-D helical phase of encapsulated guest molecules have been observed in SWCNTs with different distributions of tube diameters [15-19]. Similarly, studies of atomic crystals formed inside nanotubes have also attracted considerable attention due to their novel electronic and structural properties [20-24]. Atomic chain structures, which are absent in its bulk phase, can be fabricated in the 1-D confined channel of macromolecules. Studies such as the growth of linear carbon chains inside nanotube/iodine chains inside AlPO4 molecules have been performed in both experiment and theory [25-29]. Recent experimental progress is encouraging. A novel double helical chain organized using iodine atoms (the so-called helical I-chain) has been produced inside SWCNTs [30]. Theoretical analysis indicates that the charge transfer from the tube to the I-chain is responsible for its stability. The study also indicates that the observed different periodicities of I-chains are induced by the different chirality of the tubes. Another experimental study shows that single, double and triple helical I-chain structures can be stable inside SWCNTs when the diameter matches a certain size [31]. For a diameter larger than 1.45 nm, the chain structure decomposes and crystalizes into the bulk phase, which indicates there is a critical size of the hollow nanospace for a stable formation of I-chains. Undoubtedly, these studies open a pathway for the exploration and design of new material structures within confining 1-D nanospace.

Similar to the structure of CNTs, boron nitride nanotubes (BNTs) are also rolled up using a hexagonal sheet, but they are constructed by alternating boron and nitrogen atoms. BNTs exhibit some superior properties compared to CNT, such as much higher chemical and thermodynamic stability [32, 33]. Due to their unique hollow structure, BNTs can also be used as the host molecule to prepare a hybrid peapod by filling it with various guest molecules. A theoretical study indicates that BNTs are more suitable to prepare peapod systems than CNTs with the same chiral index. This is because much energy can be gained upon encapsulation [34]. *Ab-initio* calculation shows that the doped C_{60} molecule with a potassium atom inside BNTs can induce a significantly higher density of electronic states at the Fermi level than any of the currently available C_{60} crystals can. This makes the BNT-peapod structure a promising material to study superconducting properties in fullerene-based materials [35]. High-resolution transmission electron microscopy (HRTEM) images show that the encapsulated C_{60} molecules inside single-

Author α ρ ω: College of Science, Liaoning University of Technology, Jinzhou, Liaoning, 121001, China. e-mail: yaozhenjlu@163.com
Author σ: College of Mathematics and Physics, Bohai University, Jinzhou, Liaoning, 121000, China.
Author ¥: Mechannical Engineering and Automation College, Liaoning University of Technology, Jinzhou, Liaoning, 121001, China.

walled boron-nitride nanotubes (SWBNTs) also exhibit ordered phases similar to the C_{60}@SWCNT peapod systems. However, there are different stacking configurations for the same tube diameter [36]. The strikingly different properties of BNTs compared to CNTs offers great promise for applications in future molecular electronic devices. From the studies mentioned above, we know that novel single, double, and triple helical I-chains can be produced inside SWCNTs with a certain size of diameter. However, no theoretical or experimental study of a helical I-chain inside BNTs has been reported up to now. We also study how the tube diameter and chirality affect the stability of encapsulated I-chains. Thus, this detailed analysis of stable structures of encapsulated helical I-chains inside SWBNTs may open new insights and further possibilities for applications.

In the present work, the single, double, and triple helical I-chains were constructed inside different SWBNTs. This study focuses on the helicity (including the helical radius and helical angle) of stable helical I-chains inside SWBNTs for different diameters and chirality. We use the Lanner-Jones 12-6 potential function to describe the systematic van der Waals interaction. The results show that the optimal helical radius, opt(r), of encapsulated helical I-chains increases linearly with the tube radius (R_T), which produces a constant gap (~3.7-3.9 Å) between the I-chain and the tube wall. The optimal helical angle, opt(φ), cannot be determined for a single helical I-chain due to the lack of inter-chain interaction. For the investigated double and triple helical I-chains, a small opt(φ) can be induced using large inter-chain for the same tube or a large tube for the same chain structure. The comparative analysis indicates that the helicity of a stable helical I-chain is insensitive to tube chirality, but it depends on the tube diameter. This study aims to better understand the competing mechanism of chain/tube interaction and inter-chain interaction on the helicity of stable helical I-chains inside SWBNTs.

II. Model and Simulation Method

For the simulation of the I-chain@SWBNTs peapod system, we position the tube in a Cartesian coordinate system with its center of mass as the origin *O*. As shown in Fig.1, the tube's long axis coincides with the *OZ*-axis with its length exceeding 1200 Å. This is long enough for the longest helical I-chain (~1100 Å) we use in this study. Thus, the systematic edge effect can be ignored. In the *O-XY* projection plane, two circles with the radius R_T and r correspond to the cross section of SWBNT and the growth trajectory of the chain structures, respectively. The black, red, and purple solid points stand for the iodine atoms of single, double, and triple helical chains, respectively. Because the coordinates of a single helical chain coincide with the coordinates of the first chain structure of double and triple helical chains, the atoms of single helical chains are shown with mixed colors. For a given helical radius r, the initial coordinates for the chain structures can be defined as ($r\cos\varphi_0$, $r\sin\varphi_0$, 0) with the initial helical angle $\varphi_0=(n-1)2\pi/m$. Here, parameter m =1, 2, and 3 stand for the type of helical chain, and the parameter n (which ranges from 1 to m) stands for the nth chain. For a given φ, the total number of atoms in a single chain structure can be obtained using $N=2\pi/\varphi$ with N being an integer. The length of a complete periodic structure is determined by $L=N(d^2-(2r\sin(\varphi/2))^2)^{1/2}$ with the bonding length (d) of the I-chains set as 2.9 Å, based on Refs. 30. Thus, the spatial positions of arbitrary iodine atoms in each chain structure are defined using the coordinates $(r\cos(\varphi_0+k\varphi), r\sin(\varphi_0+k\varphi), k(d^2-(2r\sin(\varphi/2))^2)^{1/2}-L/2)$ with the parameter k =0, 1, 2, 3, … (N -1). Due to the square root $d^2-(2r\sin(\varphi/2))^2$ of the z coordinate should be equal to or larger than zero, the maximum value of φ for the fixed r and d of a helical chain is given by equation (1).

$$0\le\varphi\le 2\arcsin(d/2r) \tag{1}$$

Similar to the fullerene peapod system, a systematic interaction such as the interaction between the I-chains and tubes (referred to as chain/BNT interaction) as well as the internal interaction between two I-chains (referred to as inter-chain interaction) are due to the van der Waals interaction given by the Lennard-Jones 12-6 potential. The total interaction energy $V(R_T, r, \varphi)$ of the single, double, and triple helical I-chain peapod system, with a given R_T, r, and φ, can be obtained using the nanotube field potential given by equations (2-4).

$$V(R_T, r, \varphi)_{\text{Single}} = \sum_{N_\tau}\sum_{N_{\lambda 1}} v\left(|\rho_\tau - \rho_{\lambda 1}|\right) \tag{2}$$

$$\begin{aligned} V(R_T, r, \varphi)_{\text{Double}} &= \sum_{N_\tau}\sum_{N_{\lambda 1}} v\left(|\rho_\tau - \rho_{\lambda 1}|\right) \\ &+\sum_{N_\tau}\sum_{N_{\lambda 2}} v\left(|\rho_\tau - \rho_{\lambda 2}|\right) + \sum_{N_{\lambda 1}}\sum_{N_{\lambda 2}} v\left(|\rho_{\lambda 1} - \rho_{\lambda 2}|\right) \end{aligned} \tag{3}$$

$$\begin{aligned} V(R_T, r, \varphi)_{\text{Triple}} &= \sum_{N_\tau}\sum_{N_{\lambda 1}} v\left(|\rho_\tau - \rho_{\lambda 1}|\right) \\ &+\sum_{N_\tau}\sum_{N_{\lambda 2}} v\left(|\rho_\tau - \rho_{\lambda 2}|\right) + \sum_{N_\tau}\sum_{N_{\lambda 3}} v\left(|\rho_\tau - \rho_{\lambda 3}|\right) \\ &+\sum_{N_{\lambda 1}}\sum_{N_{\lambda 2}} v\left(|\rho_{\lambda 1} - \rho_{\lambda 2}|\right)+\sum_{N_{\lambda 1}}\sum_{N_{\lambda 3}} v\left(|\rho_{\lambda 1} - \rho_{\lambda 3}|\right) \\ &+\sum_{N_{\lambda 2}}\sum_{N_{\lambda 3}} v\left(|\rho_{\lambda 2} - \rho_{\lambda 3}|\right) \end{aligned} \tag{4}$$

The parameters τ and λ (λ1, λ2, and λ3) correspond to the atoms of BNT and the helical I-chain, respectively. Here, ρ_i and N_i (i=τ and λ) index the coordinates and the number of corresponding atoms. Since the total number of atoms in a single chain structure depends on the variable parameter φ, the monatomic interaction energy, $V(R_T, r, \varphi)_{atom}$, which gives the average interaction energy for a single iodine atom, can be calculated for a simple analysis using equation (5).

$$V(R_T, r, \varphi)_{atom} = V(R_T, r, \varphi)/mN. \quad (5)$$

The Lennard-Jones 12-6 potential used in the calculation is given in equation (6).

$$v(r)=D_{IJ}(-2(R_{IJ}/r)^6+(R_{IJ}/r)^{12}) \quad (6)$$

The potential parameters for the van der Waals distance RIJ and energy DIJ are listed in Table I [37]. This interaction potential has been used, widely and successfully, to study different interacting peapod systems [38-40].

The helical I-chains only stabilize for a radius smaller than 7.25 Å when filled into the CNTs - according to a previous study [31]. BNTs that include three armchair tubes and sixteen achiral tubes with R_T ranging from 6.905 Å to 8.435 Å are selected for the study. This radius distribution range is slightly larger than for CNTs due to a larger confinement effect produced by the BNTs [39]. Detailed structural information of the BNTs is listed in Table II. The calculation is performed as described in the following steps. For a fixed tube with a given R_T, the r of the helical I-chain changes from 1.5 Å to R_T with the step size Δr =0.1 Å. The φ begins at 1° and increases with a step size $\Delta\varphi=1°$ to the maximum defined in Equation (1). For each increase of r or φ, a complete period of the helical chain (with m =1, 2 and 3 corresponding to the single, double and triple helical chains, respectively) is obtained with the calculation. Then, the systematical interaction energies $V(R_T, r, \varphi)_{atom}$ for the constructed single, double, and triple helical chain peapod systems can be obtained using the equations (2-4), and combining equations (5-6). Thus, opt(r) and opt(φ), which correspond to the most stable helical chain for a given R_T, can be determined using the obtained minimum interaction energy.

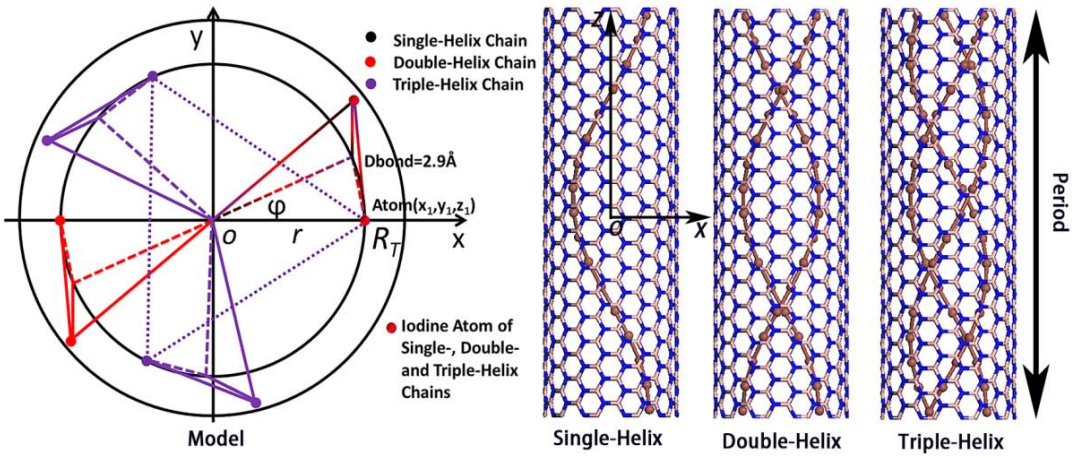

Fig. 1: Image of the constructed model in a Cartesian coordinate system. Parameters r and φ correspond to the helical radius and helical angle of the I-chain for a given tube radius R_T. The atoms of the single, double, and triple helical chains are colored as black, red, and purple, respectively

Table 1: The L-J 12-6 potential parameters for I-I, I-N, and I-B used in this study

Type	I-I	I-N	I-B
DIJ	0.339	0.153	0.247
RIJ	4.50	4.08	4.292

III. Results and Discussions

Two equations are addressed in this section. One is the optimal helicity (including opt(r) and opt(φ)) of encapsulated single, double and triple helical chains inside different SWBNTs. The other is the mechanism of the influence of the tube's confinement effect (or chain-BNT interaction: including the diameter and chirality) and the inter-chain interaction on the helicity of a stable helical chain. Firstly, we select the minimum (10, 10) armchair tube as an example to determine the opt(r) and opt(φ) of the encapsulated three constructed helical chains by calculating the systematic interaction energies (V_{atom}). In Fig.2 we can see that the opt(r) values that correspond to the minimum value of V_{atom} for single, double, and triple helical chains. They are 3.1 Å, 3.0 Å and 3.1 Å, respectively. The similar opt(r) obtained here lead to a similar distance (~3.8 Å-3.9 Å)

between the tube's wall and the helical chain, which is in good agreement with the reported experimental results [30, 31]. Similarly, the V_{atom}-φ curves of three constructed helical chains are presented in Fig.3. It can be seen that the V_{atom} of a single helical chain is generally invariant with the increased φ, which means there is an insensitive dependency between them. For the presented results of double and triple helical chains, the V_{atom} exhibits a generally invariant and decreased tendency with φ for the low and high angle region. The obtained opt(φ) values, which correspond to the minimum value of V_{atom} of double and triple helical chains are 50° and 40°, respectively. The V_{atom} of a single helical chain only considers the chain/BNT interaction, while the V_{atom} of the double and triple helical structures considers both the chain/BNT interaction and the inter-chain interaction. Consequently, the exhibited different V_{atom}-φ behavior of the single helical structure from the double and triple helical chains must be due to the absence of inter-chain interaction. In particular, opt(φ) can be determined only for the case where inter-chain interaction is considered for the chain structures parameter $m \geq 2$. However, the results above only show the importance of inter-chain interaction to determine opt(φ). No direct evidence is confirmed for whether the tube's confinement effect can affect opt(φ) or not. A more detailed discussion of this open question is below.

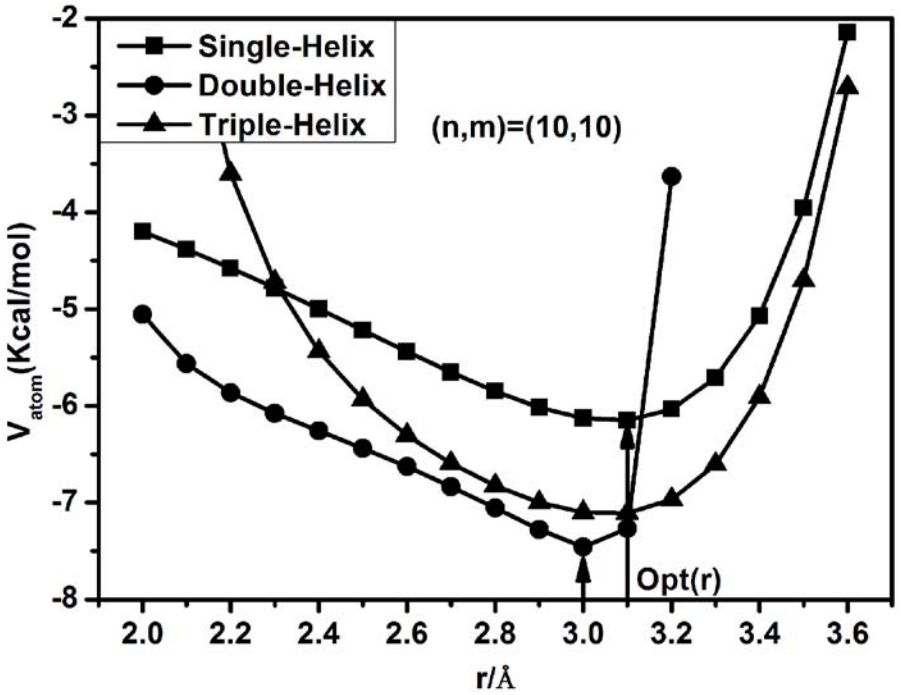

Fig. 2: Systematic interaction energies (V_{atom}) as a function of helical radius (r) for the select armchair (10, 10) tube. The square, circular, and triangular solid points correspond to the V_{atom} of single, double and triple helical chains, respectively

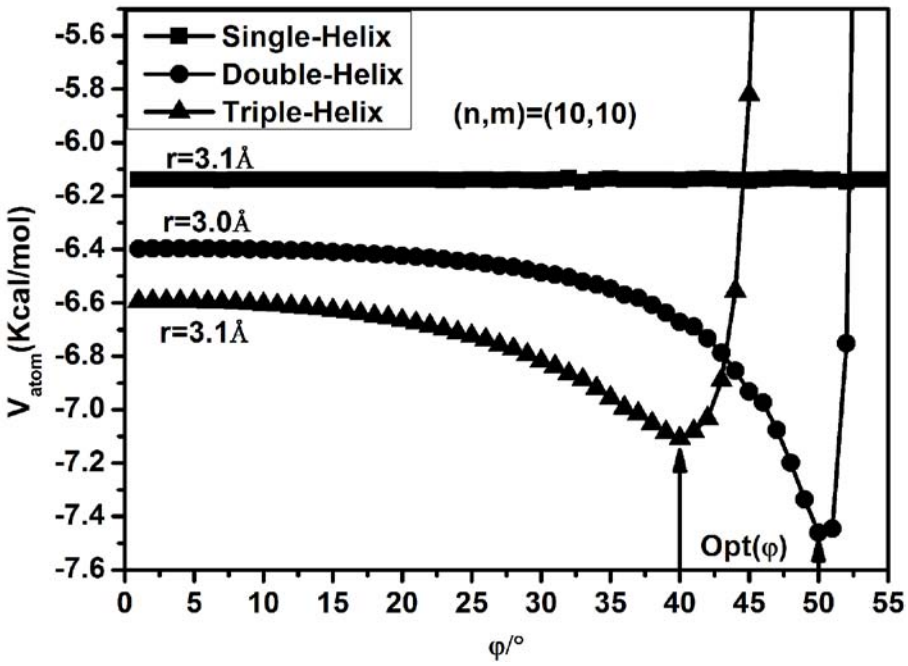

Fig. 3: Systematic interaction energies (V_{atom}) as a function of the helical angle (φ) for the select armchair (10, 10) tube with the corresponding opt(r) is fixed. The square, circular, and triangular solid points correspond to the V_{atom} of single, double, and triple helical chains, respectively

All calculated results, including opt(r), the distance between iodine chains and tube's wall (space), and opt(φ) are listed in Table II. For an intuitive analysis, the opt(r)-R_T and space-R_T, and opt(φ)-R_T are presented in Fig.4 and Fig.5, respectively. Moreover, some optimal double and triple helical chains are shown in Fig.7 and Fig.8. We can see that the opt(r) of single helical chain increases linearly from 3.1 Å to 4.6 Å as R_T increases from 6.905 Å to 8.435 Å. Similarly, opt(r) of double and triple helical chains increases linearly from 3.0 Å to 4.6 Å, and from 3.1 Å to 4.7 Å, respectively, for the same interval of R_T like the single helical chain (see Fig.7 and Fig.8). The obtained identical increasing tendency of opt(r) for the single helical structure as the studied double and triple helical chains (considering the different interactions between them) indicates that opt(r) mainly depends on the tube's confinement effect. The tube's confinement effect is associated with the tube diameter and chirality. It can be seen that some small platforms, which correspond to the same opt(r) for a similar R_T but different chirality, are visible in Fig.4. This indicates that opt(r) is insensitive to the tube's chirality but strongly depends on the tube diameter. Additionally, a similar distance (~3.7 Å to 3.9 Å) between the chain structure and tube's wall is obtained for these three helical chains, which is consistent with reported experimental results [30, 31]. The small fluctuations for the obtained distance (~3.7 Å to 3.9 Å) here are caused by the calculation accuracy of Δr=0.1 Å. A more uniform space should be produced by using a smaller value for Δr such as 0.01 Å or 0.001 Å. It is, however, impractical because the calculation is complex and expensive.

Since opt(φ) can not be determined for a single helical chain structure due to the absence of inter-chain interaction, we only show the opt(φ)- R_T curves for double and triple helical chains - see Fig.5. It can be seen that the double helical chain exhibits a larger opt(φ) than the triple helical chain when they were filled into the same tubes. Additionally, the obtained opt(φ) decreases, in general, from 50° to 35°, and from 40° to 32° for the double and triple helical chain, respectively (see Fig.7 and Fig.8). The obtained different opt(φ), but identical variation tendency as R_T for the double and triple chains, can be interpreted as follows. For the same tube, similar opt(r) values are obtained for the double and triple helical chains. However, a larger inter-chain interaction, due to a smaller inter-chain distance, can be produced for the triple helical chain than by encapsulating the double helical chain. Thus, the large inter-chain interaction can induce a small opt(φ). On the other hand, for the same chain structure with different tubes, the decreased value of opt(φ) as the increased R_T shows that a large tube with a small confinement effect can induce a small helical angle. More specifically, opt(φ) shows an inverse proportional relationship with the inter-chain interaction for the same tubes. However, a direct proportional relationship between opt(φ) and the tube's confinement effect is observed for the same chain structures. Similarly, some

small platforms, i.e. the same opt(φ) for similar R_T but different chirality, are also shown in Fig.5. This indicates that opt(φ) is insensitive to the tube's chirality, but it depends on the tube diameter. A similar conclusion has been reported for the case of encapsulated C_{60} molecules inside carbon nanotubes, where the stable orientation mainly depends on the tube diameter [41]. The periodic length *L* of the obtained optimal helical structures is shown in Fig.6. The periodic length *L* of double and triple helical chains decreases generally with increasing R_T (see Fig.7 and Fig.8). This can be interpreted as the expression $L=N(d^2-(2r\sin(\varphi/2))^2)^{1/2}$ where the period *L* obeys an inverse relationship with the variables φ and r for the invariable d. Thus, the competing relationship of an increasing r and decreasing φ causes the *L* to decrease with R_T. In comparison, the *L* of the triple helical chain is larger than the double helical chain for the same R_T /similar opt(r). This is because a smaller opt(φ) is obtained for the triple helical chain.

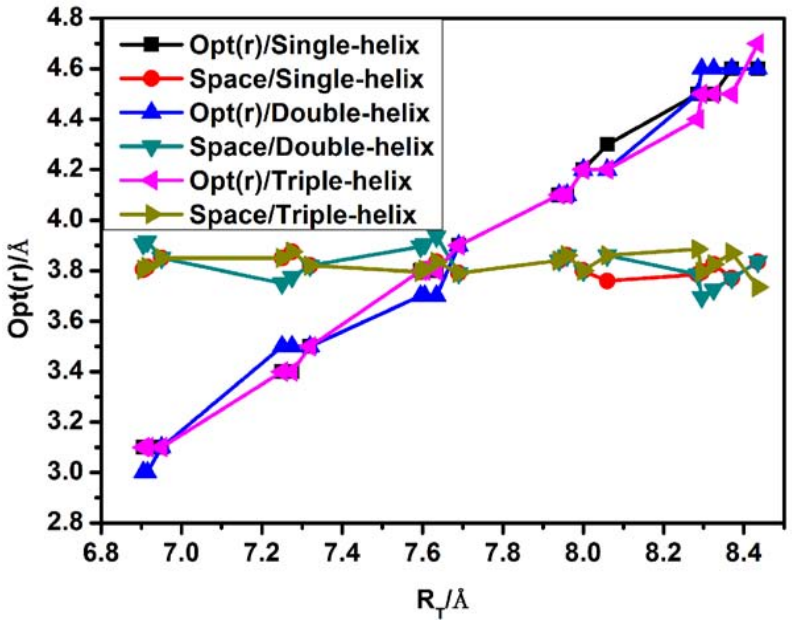

Fig. 4: Values for opt(r) and the distance between the I-chains and tube wall for three studied helical chains, as a function of the tube radius R_T

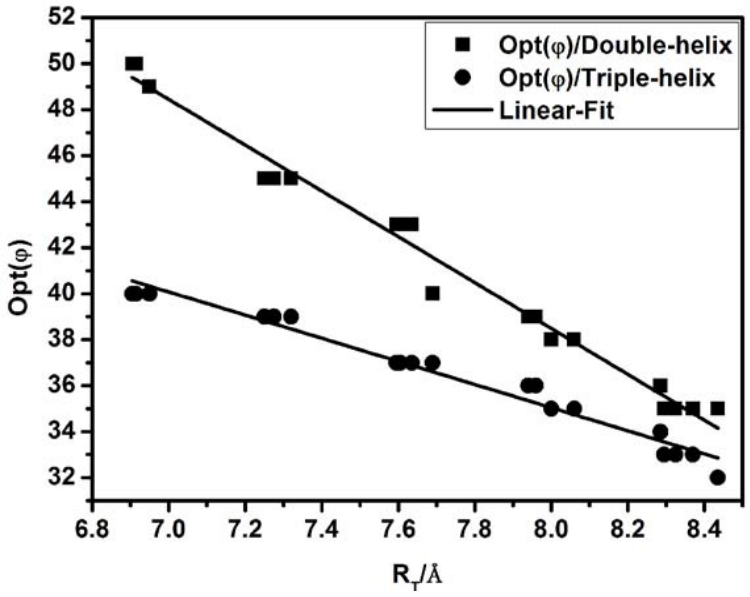

Fig. 5: The opt(φ) values for double (squares) and triple (circles) helical chains, as a function of the tube radius R_T. The linear fits are shown as a guide for the eye

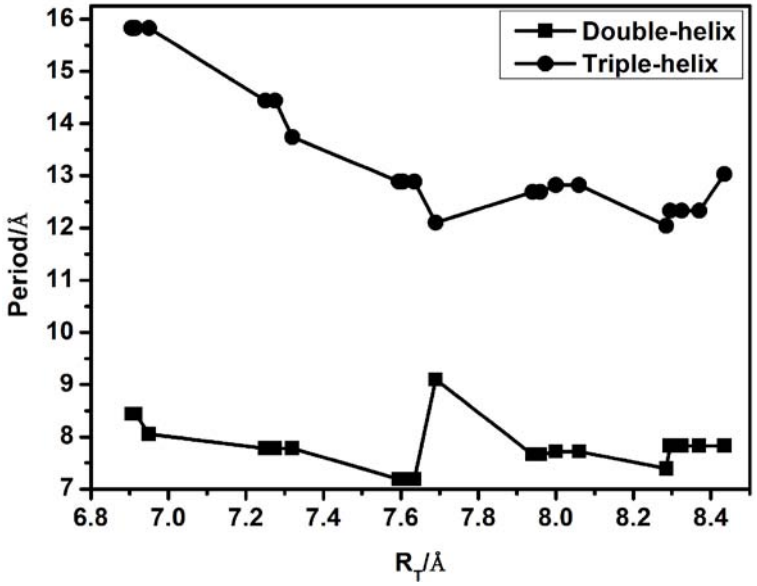

Fig. 6: The length of the periodic length unit *L* for optimal double (squares) and triple (circles) helical chains, as a function of the tube radius R_T

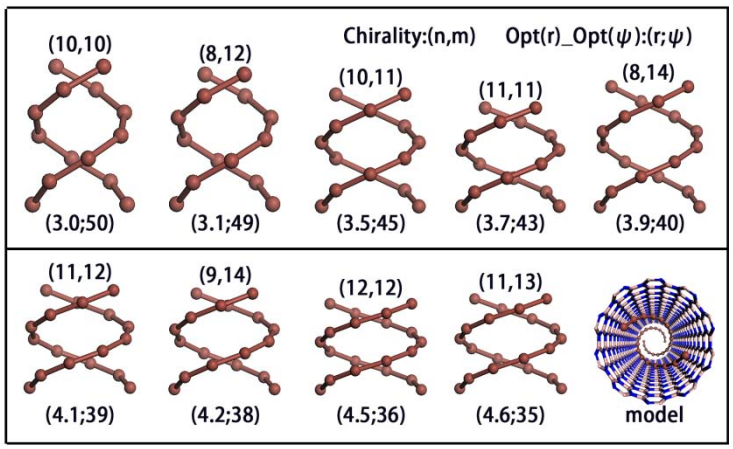

Fig. 7: Illustration of some optimal double helical chains as shown in Fig.4 and Fig.5. The tube's chiral index (n, m) and opt(*r*)_opt(φ) are labeled at the top and bottom, respectively

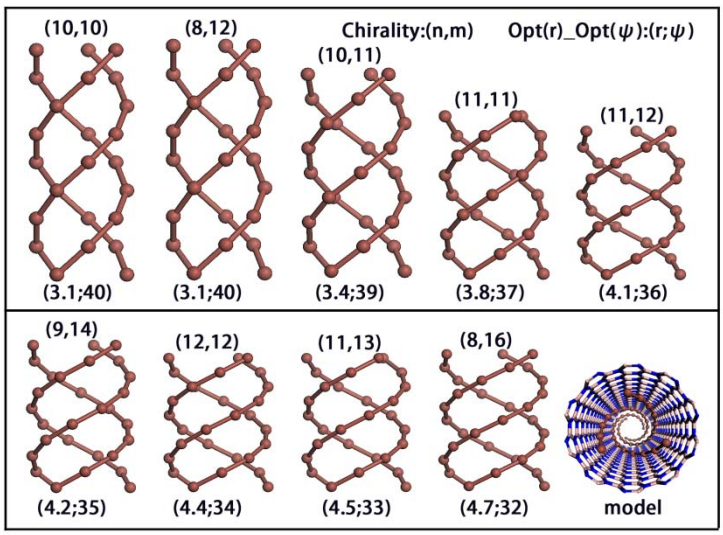

Fig. 8: Similar illustrations as in Fig.7 but for the triple helical chain

Table II. Detailed structural properties of SWBNTs and the calculated results in this study. Columns I and II show the tube's chirality and radius, respectively. Columns III and IV show the optimal helical radius and space for a single helical chain, respectively. Columns V-VII and VIII-X show the optimal helical radius, the space, the optimal helical angle of double and triple helical chains, respectively.

Table 2

(n,m)	R_T/Å	Single Helix		Double Helix			Triple Helix		
		Opt(*r*)/Å	Space/Å	Opt(*r*)/Å	Space/Å	Opt(φ)/°	Opt(*r*)/Å	Space/Å	Opt(φ)/°
(10,10)	6.905	3.1	3.805	3.0	3.905	50	3.1	3.805	40
(9,11)	6.915	3.1	3.815	3.0	3.915	50	3.1	3.815	40
(8,12)	6.95	3.1	3.85	3.1	3.85	49	3.1	3.85	40
(10,11)	7.25	3.4	3.85	3.5	3.75	45	3.4	3.85	39
(9,12)	7.275	3.4	3.875	3.5	3.775	45	3.4	3.875	39
(8,13)	7.32	3.5	3.82	3.5	3.82	45	3.5	3.82	39
(11,11)	7.595	3.8	3.795	3.7	3.895	43	3.8	3.795	37
(10,12)	7.605	3.8	3.805	3.7	3.905	43	3.8	3.805	37
(9,13)	7.635	3.8	3.835	3.7	3.935	43	3.8	3.835	37
(8,14)	7.69	3.9	3.79	3.9	3.79	40	3.9	3.79	37
(11,12)	7.94	4.1	3.84	4.1	3.84	39	4.1	3.84	36
(10,13)	7.96	4.1	3.86	4.1	3.86	39	4.1	3.86	36
(9,14)	8.00	4.2	3.8	4.2	3.8	38	4.2	3.8	35
(8,15)	8.06	4.3	3.76	4.2	3.86	38	4.2	3.86	35
(12,12)	8.285	4.5	3.785	4.5	3.785	36	4.4	3.885	34
(11,13)	8.295	4.5	3.795	4.6	3.695	35	4.5	3.795	33
(10,14)	8.325	4.5	3.825	4.6	3.725	35	4.5	3.825	33
(9,15)	8.37	4.6	3.77	4.6	3.77	35	4.5	3.87	33
(8,16)	8.435	4.6	3.835	4.6	3.835	35	4.7	3.735	32

IV. Conclusions

In summary, this study comprises a simulation of encapsulated single, double, and triples helical I-chains inside SWBNTs with different diameters and chirality distributions. We focused on the helicity of stable helical I-chains and their formation mechanism inside SWBNTs by calculating the interaction energy using the van der Waals potential. The results show that the optimal helical radius, opt(*r*), of encapsulated I-chains increases linearly with the tube radius (R_T), which produces a constant distance (~3.7-3.9 Å) between the I-chain and the tube wall. The optimal helical angle, opt(φ), can not be determined for a single helical I-chain due to the lack of inter-chain interaction. The opt(φ) for the double helical chain is larger than the value for the triple helical chain when they are filled into the same tubes. This is because the larger inter-chain interaction can induce a smaller opt(φ). The obtained opt(φ) for double and triple helical I-chains decreases linearly with increasing R_T because the large tubes can induce a small opt(φ). The comparative analysis indicates that the helicity of stable I-chain structures is insensitive to the tube's chirality, but it strongly depends on the tube diameter. Additionally, the periodic length *L* for the triple helical chain is larger than for double helical chain for the same R_T and similar opt(r). This is because a smaller opt(φ) is obtained for the triple helical chain. This work not only provides images of the structure of encapsulated double and triple helical I-chains inside SWBNTs, but also reveals the formation mechanism for stable helical structures.

V. Acknowledgement

This work was supported financially by the National Natural Science Foundation of China under Grant Nos 11504150.

References Références Referencias

1. B. W. Smith, M. Monthioux and D. E. Luzzi, Encapsulated C60 in carbon nanotubes, *Nature* 1998, 396, 323-324.
2. L. C. Qin, Determination of the chiral indices (n,m) of carbon nanotubes by electron diffraction, *Phys. Chem. Chem. Phys.* 2007, 9, 31-48.
3. S. Iijima, Helical microtubules of graphitic carbon, *Nature* 1991, 354, 56-58.
4. Z. D. Liu, M. G. Yao, Y. Yuan, S. L. Chen, R. Liu, S. C. Lu, B. Zou, T. Cui and B. B. Liu, Raman spectroscopy of bromine chains inside the one-dimensional channels of AlPO4-5 single crystals, *J. Raman Spectrosc.* 2015, 46, 413-417.
5. Z. X. Zhang, Z. Y. Pan, Q. Wei, Z. J. Li, L. K. Zang and Y. Z. Wang, Mechanics of nanotubes filled with C60, C36 and C20, *International Journal of Modern Physics* B 2003, 17, 4667-4674.
6. J. Lu, S. Nagase, S. Re, X. W. Zhang, D. P. Yu, J. Zhang and R. Han, Interplay of single-wall carbon nanotubes and encapsulated La@C_{82}, La2@C_{80}, and Sc_3N@C_{80}, *Phys. Rev. B* 2005, 71, 235417.

7. L. H. Guan, Z. J. Shi, M. X. Li and Z. N. Gu, Ferrocene-filled single-walled *carbon* nanotubes, Carbon 2005, 43, 2780-2785.
8. K. Koga, G. T. Gao, H. Tanaka and X. C. Zeng, Formation of ordered ice nanotubes inside carbon nanotubes, *Nature* 2001, 412, 802-805.
9. R. R. Meyer, J. Sloan, R. E. D. Borkowski, A. I. Kirkland, M. C. Novotny, S. R. Bailey, J. L. Hutchison and M. L. H. Green, Discrete atom imaging of one-dimensional crystals formed within single-walled carbon nanotube, *Science* 2000, 289, 1324-1326.
10. B. Burteaux, A. Claye, B. W. Smith, M. Monthioux, D. E. Luzzi and J. E. Fischer, Abundance of encapsulated C_{60} in single-wall carbon nanotubes, *Chem. Phys. Lett. 1999*, 310, 21-24.
11. B. H. Shiozawa, T. Pichler, A. Gruneis, R. Pfeiffer, H. Kuzmany, Z. Liu, K. Suenaga and H. Kataura, A catalytic reaction inside a single-walled carbon nanotube, *Adv. Mater.* 2008, 20, 1443-1449.
12. S. Okada, M. Otani and A. Oshiyama, Electron-state control of carbon nanotubes by space and encapsulated fullerenes, *Phys. Rev.* B 2003, 67, 205411.
13. T. Miyake and S. Saito, Electronic structure of C_{60}-encapsulating semiconducting carbon nanotube, *Solid state communications* 2003, 125, 201-204.
14. Z. Zhou, J. J. Zhao, P. V. R. Schleyer and Z. F. Chen, Insertion of C_{50} into single-walled carbon nanotubes: selectivity in interwall spacing and C_{50} isomers, *J. Comput. Chem*. 2008, 29, 781-787.
15. A. N. Khlobystov, D. A. Britz and G. A. D. Briggs, Molecules in carbon nanotubes, *Acc. Chem. Res.* 2005, 38, 901-909.
16. M. Hodak and L. A. Girifalco, Ordered phases of fullerne molecules formed inside carbon nanotubes, *Phys. Rev. B* 2003, 67, 075419.
17. K. S. Troche, V. R. Coluci, S. F. Braga, D. D. Chinellato, F. Sato, S. B. Legoas, R. Rurali and D. S. Galvao, Prediction of ordered phases of encapsulated C_{60}, C_{70}, and C_{78} inside carbon nanotubes, *Nano lett.* 2005, 5, 349-355.
18. A. N. Khlobystov, D. A. Britz, A. Ardavan and G. A. D. Briggs, Observation of Ordered Phases of Fullerenes in Carbon Nanotubes, *Phys. Rev. Lett.* 2004, 92, 245507.
19. S. B. Legoas, R. P. B. D. Santos, K. S. Troche, V. R. Coluci and D. S. Galvao, Ordered phases of encapsulated diamondoids into carbon nanotubes, *Nanotechnology*, 2011, 22, 315708.
20. J. Sloan, S. J. Grosvenor, S. Friedrichs, A. I. Kirkland, J. L. Hutchison and M. L. H. Green, A one-dimensional BaI2 chain with five- and six-coordination, formed within a single-walled carbon nanotube, *Angew. Chem. Int. Ed.* 2002, 41, 1156-1159.
21. J. Sloan, M. Terrones, S. Nufer, S. Friedrichs, S. R. Bailey, H. G. Woo, M. Ruhle, J. L. Hutchison and M. L. H. Green, *J. AM. CHEM. SOC.* 2002, 124, 2116-2117.
22. S. P. Huang, W. D. Cheng, J. M. Hu, Z. Xie, H. Hu and H. Zhang, A periodic density functional theory study on the effects of halides encapsulated in SiC nanotubes, *J. Chem. Phys.* 2008, 129, 174108.
23. C. Xu, J. Sloan, G. Brown, S. Bailey, V. C. Williams, S. Friedrichs, K. S. Coleman, E. Flahaut, J. L. Hutchison, R. E. D. Borkowski and M. L. H. Green, 1D lanthanide halide crystals inserted into single-walled carbon nanotubes, *Chem. Commun.* 2000, 2427-2428.
24. J. Sloan, M. C. Novotny, S. R. Bailey, G. Brown, C. Xu, V. C. Williams, S. Friedrichs, E. Flahaut, R. L. Callender, A. P. E. York, K. S. Coleman, M. L. H. Green, R. E. D. Borkowski and J. L. Hutchison, Two layer 4:4 co-ordinated KI crystals grown within single walled carbon nanotubes, *Chem. Phys. Lett.* 2000, 329, 61-65.
25. C. Zhao, R. Kitaura, H. Hara, S. Irle and H. Shinohara, Growth of linear carbon chains inside thin double-wall carbon nanotubes, *J. Phys. Chem.* C 2011, 115, 13166-13170.
26. X. L. Zhao, Y. Ando, Y. Liu, M. Jinno and T. Suzuki, Carbon nanowire made of a long linear carbon chain inserted inside a multiwalled carbon nanotube, *Phys. Rev. Lett.* 2003, 90, 187401.
27. Y. Liu, R. O. Jones, X. L. Zhao and Y. Ando, Carbon species confined inside carbon nanotubes: A density functional study, *Phys. Rev. B* 2003, 68, 125413.
28. J. T. Ye, Z. K. Tang and G. G. Siu, Optical characterizations of iodine molecular wires formed inside the one-dimensional channels of an AlPO4-5 single crystal, *Appl. Phys. Lett.* 2006, 88, 073114.
29. J. M. Hu, J. P. Zhai, F. M. Wu and Z. K. Tang, Molecular dynamics study of the structures and dynamics of the iodine molecules confined in AlPO4-11 crystals, *J. Phys. Chem. B* 2010, 114, 16481-16486.
30. X. Fan, E. C. Dickey, P. C. Eklund, K. A. Williams, L. Grigorian, R. Buczko, S. T. Pantelides and S. J. Penycook, Atomic arrangement of iodine atoms inside single-walled carbon nanotubes, *Phys. Rev. Lett.* 2000, 84, 4621-4624.
31. L. Guan, K. Suenaga, Z. J. Shi, Z. N. Gu and S. Iijima, Polymorphic structures of iodine and their phase transition in confined nanospace, *Nano Lett.* 2007, 7, 1532-1535.
32. F. X. Ma, Z. Yao, M. G. Yao, R. Liu, T. Cui and B. B. Liu, Tubular shape fullerenes inside single wall boron nitride nanotubes: a theoretical simulation, *J. Nanosci. Nanotechnol.* 2016, 16, 5776-5781.
33. Z. Yao, J. Y. Lv, C. J. Liu, H. Lv and B. B. Liu, Preferable orientations of interacting C60 molecules inside single wall boron nitride nanotubes, *Chin. Phys. Lett.* 2016, 33, 056701.

34. S. Okada, S. Saito and A. Oshiyama, Semiconducting form of the first-row elements: C_{60} chain encapsulated in BN nanotubes, *Phys. Rev. B* 2001, 64, 201303.
35. V. Timoshevskii and M. Cote, Doping of C60-induced electronic states in BN nanopeapods: Ab initio simulations, *Phys. Rev. B* 2009, 80, 235418.
36. W. Michelson, S. Aloni, W. Q. Han, J. Cumings and A. Zettl, Packing C_{60} in boron nitride nanotubes, *Science* 2003, 300, 467-469.
37. A. K. Rappe, C. J. Casewit, K. S. Colwell, W. A. Goddard and W. M. Skiff, UFF, a full periodic table force field for molecular mechanics and molecular dynamics simulations, *J. Am. Chem. Soc.* 1992, 114, 10024-10035.
38. B. Verberck and K. H. Michel, Nanotube field and orientational properties of C70 molecules in carbon nanotubes, *Phys. Rev. B* 2007, 75, 045419.
39. F. X. Ma, Z. Yao, M. G. Yao, R. Liu, B. Zou, T. Cui and B. B. Liu, Preferable orientation of spherical fullerene inside boron nitride nanotubes, *J. Phys.: Condensed Matter,* 2013, 25, 065402.
40. Z. Yao, R. Liu, F. X. Ma, S. C. Lu, F. B. Tian, D. F. Duan, T. Cui and B. B. Liu, Preferred orientations of encapsulated C_{60} molecules inside single wall carbon nanotubes, *Chin. Phys. B* 2013, 22, 076101.
41. B. Verberck and K. H. Michel, Nanotube field of C60 molecules in carbon nanotubes: atomistic versus continuous approach, *Phys. Rev. B* 2006, 74, 045421.